Non-conservative sandpile cellular automaton on the Bethe lattice

1995 J. Phys. A: Math. Gen. 28 6903

(http://iopscience.iop.org/0305-4470/28/23/030)

J. Phys. A: Math. Gen. 28 (1995) 6903–6914. Printed in the UK

Non-conservative sandpile cellular automaton on the Bethe lattice

Mária Markošová†

Institute of Measurement Science, Slovak Academy of Sciences, Dúbravská 9, Bratislava, Slovak Republic

Received 19 May 1995, in final form 31 July 1995

Abstract. The non-conservative noisy critical height sandpile cellular automaton with open boundary conditions is studied analytically on the Bethe lattice. Using the modified method of Dhar and Majumdar [1], the single-site probabilities, pair probabilities and the avalanche size distributions for the three versions of the automaton, with different amount of dissipated particles, are calculated.

1. Introduction

Since 1987, when Bak *et al* [2] came up with the concept of self-organized criticality (SOC), this phenomenon has been widely studied numerically [2–10], analytically [1, 11–18] and experimentally [19–21]. For the numerical and analytical studies model systems called 'sandpiles' are often used. 'Sandpiles' are cellular automata, which mimic the dynamics of the spatially extended many-particle systems with local interactions. They are defined on n-dimensional lattice (for example, a square lattice), by a starting particle distribution on its sites, by local dynamical rules, and local critical condition. They work in two dynamical modes, the first one is the input process, followed, under the certain circumstances, by the second mode, the relaxation of the system.

(i) Input mode. Equal particles (for example, sand grains of size 1 in arbitrary units) are added from outside to randomly chosen sites in the lattice. After each particle addition, the local critical condition is checked. The process continues until in any site the local critical state is reached. The local critical state can be defined, for example, by the local critical column height of particles. When the critical state has been reached, the input stops and the dynamics switches itself to the second mode.

(ii) Avalanche process. The critical site topples and the particles are distributed to sites in the neighbourhood according to the defined local dynamical rules. This also may drive the neighbours to the supercritical state and thus the avalanche may continue further in one or more directions.

It has been shown numerically, that such a dynamics drives the system to the self-organized critical state with long-range time and space correlations [2, 3], but, unlike the phase transitions, without any fine tuning of system parameters. The main indication of the SOC state is the power-law distribution of the avalanche sizes. Nature gives us a nice

† E-mail address: umermark@savba.savba.sk

manifestation of space and time-scale invariancy in the ubiquitous occurrence of fractal structures and the flicker noise phenomena. It is therefore supposed that the detailed study of systems with self-organized criticality can shed some light on the creation of the scale invariances in reality.

Sandpile cellular automata and the self-organized critical state were mainly studied numerically [2–10]. Analytical studies followed two lines:

(i) Analytical calculations on discrete systems, such as cellular automata [11–18].

(ii) Modelling of the spatially extended systems by stochastic differential equations [22, 23, 26].

The most complete analytical calculations were done for the Bak, Tang and Wiesenfeld model (BTW), that is for the critical height cellular automaton defined on a square lattice. Local distribution rules in this model affect only *nearest* neighbours of the critical site [2]. The BTW model on the Bethe lattice was treated by Dhar and Majumdar [1]. The authors succeeded in the complete analytical characterization of the self-organized critical state by single-site probabilities, pair probabilities and power-law distribution of the avalanche sizes.

By the analytical studies of the stochastic differential Langevine equation it was proved that the long-range correlations, and thus the self-organized critical state, are a consequence of the conservative dynamics, which conserves locally, and on an average, the number of particles [22, 23, 26]. On the other hand, numerical studies of non-conservative, continuously driven discrete models showed, that in the case of open boundaries, the scale invariancy exists, and the power-law scaling of avalanche sizes was found [4, 24, 25]. These models differ from the sandpile cellular automata in one crucial point. While cellular automata are noisy, and phase-space volume conserving systems, the continuously driven models (coupled map lattices) are deterministic and dissipative.

In this paper I study analytically the BTW non-conservative model on the Bethe lattice. Non-conservation is implied by the fact, that not all of the particles are distributed to the nearest neighbours, but some of them dissipate to the environment. Thus my model is a noisy, non-conservative sandpile cellular automaton. Modifying the method of Dhar and Majumdar [1], I calculated the single-site probabilities together with the avalanche size distribution, all in the final stationary state, to which the system is driven by its dynamics. My results show, that the avalanche size distributions decay exponentially and thus no SOC state exists in noisy non-conservative sandpile of BTW type with open boundaries.

2. Definition of the model and the single-site probabilities

First, I describe the dynamics of the critical height non-conservative BTW cellular automaton on the Bethe lattice. As the other sandpile models, it has two dynamical modes; the input process and the avalanche.

Input:

$$h_i \to h_i + 1 \qquad h_i < h_c \tag{1a}$$

where h_i denotes the height of the sand column at the ith site and h_c indicates the critical height.

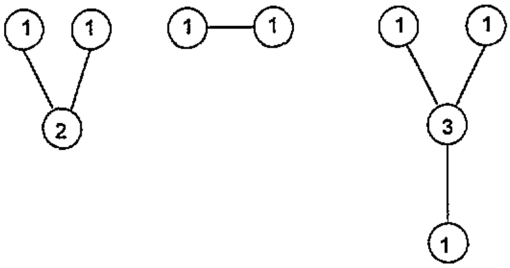

Figure 1. Three examples of disallowed configurations.

Avalanche:
If $h_i \geqslant h_c$

$$h_i \to h_i - (z + \tilde{n}) = 1 \qquad h_{nn} \to h_{nn} + 1 \tag{1b}$$

which means that z grains are distributed to the nearest neighbours nn at the Bethe lattice (in fact, z denotes the sum of nearest neighbours), $\tilde{n}$ grains dissipate to the environment, and one grain rests on the original place. The critical height h_c in (1a) and (1b) equals

$$h_c = 1 + z + \tilde{n} . \tag{1c}$$

Initial conditions are random and the boundary conditions are open. The time-scales of both processes are different. The avalanche is very quick in comparison with the time-scale of the drive.

I have studied three versions of the model (1a)–(1c), namely having $z = 3$ and $\tilde{n} = 1, 2, 3$. The model of [1] then appears as a 'conservative limit' ($\tilde{n} \to 0$). It can be seen, from the dynamics (1a)–(1c), that after the transients, in the final stationary state, one can get the one-grain configuration (e.g. one particle per site) only as a rest configuration after the toppling. Because in the final stationary state $1, 2, 3, \ldots, h_{cc} = h_c - 1$ grains per site are possible, the number of configurations equals h_{cc}^N, where N is the number of lattice sites. But some of the configurations, such as that in figure 1, are excluded. The reason is as follows. The sites with only one grain have just toppled. Therefore the previous configuration would have to contain some zero-particle sites, which is impossible [1].

In what follows, I modify the analytical method of Dhar and Majumdar developed for the conservative BTW model on the Bethe lattice [1] and calculate the single-site probabilities and the distribution function for the avalanche sizes in the case of a non-conservative model. The possibility of calculation of pair probabilities is also shown.

Let us have the Bethe tree T rooted on the vertex a. Two types of allowed configurations are defined on T; e.g.

(i) strongly allowed;
(ii) weakly allowed.

Let us imagine, that the configuration C on T is allowed and that we connect the vertex a with another site b containing only one grain figure 2. The new configuration $\tilde{C}$ arises. If $\tilde{C}$ is still allowed, the old configuration C was strongly allowed. If the new configuration $\tilde{C}$ is disallowed, the old configuration C was weakly allowed.

The number of strongly and weakly allowed configurations on the tree T is given by the equations

$$N_w(T) = \sum_{h_a=1}^{h_{cc}} N_w(T, h_a) \tag{2a}$$

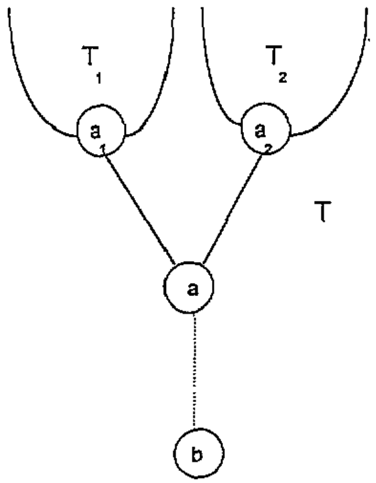

Figure 2. The definition of the strongly and weakly allowed configurations. The tree T rooted on a consists of two subtrees T_1 and T_2. Let the configuration on T be allowed. If it stays allowed also after the addition of the site b, which contains one grain, it is strongly allowed. In the opposite case it is weakly allowed.

$$N_s(T) = \sum_{h_a=1}^{h_{cc}} N_s(T, h_a). \tag{2b}$$

In equations (2a) and (2b) $N_w(T, h_a)$ and $N_s(T, h_a)$ denote the number of weakly and strongly allowed configurations on T, if on site a there is a column height h_a. If we remove the root vertex a of the tree T, it breaks into two subtrees T_1 and T_2 with vertices a_1 and a_2. Thus, if we exclude the disallowed configurations, the number of configurations $N_w(T, h_a)$, $N_s(T, h_a)$ for $h_a = 1, \ldots, h_{cc}$ is expressed as

$$N_w(T, 1) = N_s(T_1)N_s(T_2) \qquad N_s(T, 1) = 0 \tag{3a}$$

$$N_w(T, 2) = N_s(T_1)N_w(T_2) + N_w(T_1)N_s(T_2) \qquad N_s(T, 2) = N_s(T_1)N_s(T_2) \tag{3b}$$

$$\begin{aligned} N_w(T, 3) &= N_w(T_1)N_w(T_2) \\ N_s(T, 3) &= N_s(T_1)N_s(T_2) + N_w(T_1)N_s(T_2) + N_s(T_1)N_w(T_2). \end{aligned} \tag{3c}$$

To the expresions (3a)–(3c), which are also valid for the conservative case ($\tilde{n} = 0$) [1], we add another $\tilde{n}$ equations for $h_a = 4, \ldots, h_{cc}$:

$$\begin{aligned} N_w(T, h_a = 4, \ldots, h_{cc}) &= 0 \\ N_s(T, h_a = 4, \ldots, h_{cc}) &= N_s(T_1)N_s(T_2) + N_w(T_1)N_s(T_2) + N_s(T_1)N_w(T_2) \\ &\quad + N_w(T_1)N_w(T_2). \end{aligned} \tag{3d}$$

Now, the sums (2a), (2b) look like

$$N_w(T) = N_s(T_1)N_s(T_2)(1 + x_1x_2 + x_1 + x_2) \tag{4a}$$

$$N_s(T) = N_s(T_1)N_s(T_2)[(2 + x_1 + x_2) + \tilde{n}(1 + x_1 + x_2 + x_1x_2)] \tag{4b}$$

where x_i denotes the relation between the weakly and strongly allowed configurations $x_i = N_w(T_i)/N_s(T_i)$.

Let us now create the Bethe tree successively. The single site is the tree of the first generation. If we add two other sites, we get the tree of the second generation. Adding another four sites to the second generation tree one gets the tree of the third generation, etc. In this way, we create the tree of the $(m+1)$th generation from one of the mth generation. If the lattice is great ($m \to \infty$), the trees T_1, T_2 are equivalent trees of the $(m-1)$th generation. Let us denote them as $T^{(m-1)}$. Taking this into account and using the equations (4*a*), (4*b*), one gets the recursive relation

$$x^{(m+1)} = \frac{x^{(m)}+1}{\tilde{n}(x^{(m)}+1)+2}. \tag{5}$$

In equation (5), $x^{(m)}$ denotes $\frac{N_w(T^{(m)})}{N_s(T^{(m)})}$. The recursive relation (5) has one positive physically relevant fixed point x^*

$$x^* = \frac{\sqrt{(\tilde{n}+1)^2+4\tilde{n}}-(\tilde{n}+1)}{2\tilde{n}}. \tag{6}$$

With the help of x^*, we rewrite the equations (3) in the form

$$N_w(T,h_a) = \beta_w(h_a,x^*)N_s(T_1)N_s(T_2) \tag{7a}$$
$$N_s(T,h_a) = \beta_s(h_a,x^*)N_s(T_1)N_s(T_2) \tag{7b}$$

where β_w, β_s denote the coefficients, that arise for $x_1 = x^*$, $x_2 = x^*$ in a great lattice.

Using x^* equation (6), and the equations (3*a*)–(3*d*), it is easy to calculate the relations

$$\begin{aligned} N_w(T,1) &: N_w(T,2) : N_w(T,3) : N_w(T,h_a=4,\ldots,h_{cc}) \\ &: N_s(T,1) : N_s(T,2) : N_s(T,3) : N_s(T,h_a=4,\ldots,h_{cc}) \\ &= 1 : 2x^* : (x^*)^2 : 0 : 0 : 1 : 1+2x^* : (x^*+1)^2. \end{aligned} \tag{8}$$

Now we are ready to calculate the single-site height distributions, namely, the probabilities that at the randomly chosen site deep in the lattice one finds $1, 2, 3, \ldots, h_{cc}$ grains. Any site O which is somewhere far from the boundary is connected to the three trees T_1, T_2, T_3. In accordance with [1] the number of *allowed* configurations for the column height $h_O = 1, 2, 3$ is given as

$$N(T,h_O=1) = \prod_{\omega=1}^{3} N_s(T_\omega) \tag{9a}$$

$$N(T,h_O=2) = \prod_{\omega=1}^{3} N_s(T_\omega)\left[1+\sum_{j=1}^{3} x_j\right] \tag{9b}$$

$$N(T,h_O=3) = \prod_{\omega=1}^{3} N_s(T_\omega)\left[1+\sum_{j=1}^{3} x_j + \sum_{j<k} x_j x_k\right]. \tag{9c}$$

We also need $\tilde{n}$ additional expressions, namely for $h_O = 4, \ldots, h_{cc}$ which are given by the equations

$$N(T,h_O=4,\ldots,h_{cc}) = \prod_{\omega=1}^{3} N_s(T_\omega)\left[1+\sum_{j=1}^{3} x_j + \sum_{j<k} x_j x_k + x_1x_2x_3\right]. \tag{9d}$$

The site O is far from the boundary, it is therefore reasonable to use x^* instead of x_i and to rewrite (9a)–(9d) in the form

$$N(T, h_O) = \alpha(h_O, x^*) \prod_{\omega=1}^{3} N_s(T_\omega). \tag{10}$$

The total number of the allowed configurations on the lattice is given, with respect to (9a)–(9d) and (6) by the expression

$$N_{total} = \left[\varphi^2(3 + \tilde{n}\varphi)\right] \prod_{\omega=1}^{3} N_s(T_\omega) \tag{11}$$

where $\varphi = x^* + 1$. Taking into account the formulae (9)–(11), the single-site probabilities are easily calculated as

$$P(h_O, \tilde{n}) = \frac{N(T, h_O)}{N_{total}} = \frac{\alpha(h_O, \tilde{n})}{\varphi^2(3 + \tilde{n}\varphi)}. \tag{12}$$

The numerical values of the single-site probabilities for all three studied versions of (1a)–(1c) are listed in table 1 of the last section. For certain column height at the site O, the single site probability depends only on $\tilde{n}$. Putting $\tilde{n} = 0$, the single-site probabilities of the conservative automaton [1] are found.

3. Pair probabilities

The pair probability is defined as the probability of a certain column height configuration on the two distant sites in the Bethe lattice. Both sites are far from the lattice boundaries. Let us have the situation as shown in figure 3. The Bethe tree T_{k+1} rooted at the site A_{k+1} is decomposed to the tree T_k rooted on A_k and the tree U_{k+2} connected to the rest of the lattice through the site A_{k+1} [1]. According to the equations (4a) and (4b), taking into account, that the number of lattice sites tends to infinity, one gets

$$N_w(T_{k+1}) = N_s(T_k)N_s(U_{k+2}) + N_w(T_k)N_w(U_{k+2}) + N_s(T_k)N_w(U_{k+2}) + N_w(T_k)N_s(U_{k+2}) \tag{13a}$$

$$N_s(T_{k+1}) = 2N_s(T_k)N_s(U_{k+2}) + N_w(T_k)N_s(U_{k+2}) + N_s(T_k)N_w(U_{k+2}) + \tilde{n}\big[N_s(T_k)N_s(U_{k+2}) + N_w(T_k)N_w(U_{k+2}) + N_s(T_k)N_w(U_{k+2}) + N_w(T_k)N_s(U_{k+2})\big]. \tag{13b}$$

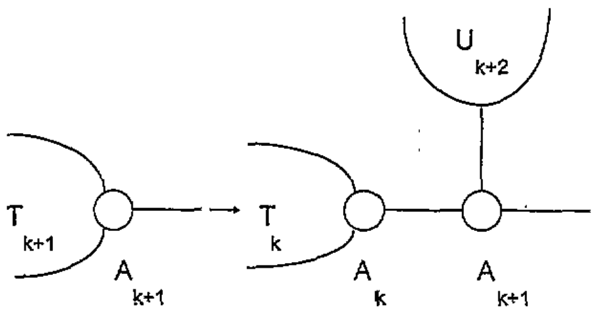

Figure 3. The recursive decomposition of the subtree T_{k+1} with the root site A_{k+1} to the subtrees T_k with root site A_k and U_{k+2}.

The matrix representation of the equations (13*a*), (3*b*) is

$$\vec{X}_{k+1} = N_s(U_{k+2})\mathbf{B}\vec{X}_k \tag{13c}$$

with $\vec{X}_k = \begin{pmatrix} N_w(T_k) \\ N_s(T_k) \end{pmatrix}$ and the matrix $\mathbf{B}$ given as

$$\mathbf{B} = \begin{pmatrix} \varphi & \varphi \\ 1+\tilde{n}\varphi & 1+(\tilde{n}+1)\varphi \end{pmatrix}. \tag{14}$$

The eigenvalues λ_1 and λ_2 and the eigenvectors $\vec{v}_1$ and $\vec{v}_2$ of the transfer matrix $\mathbf{B}$ are

$$\lambda_1 = \frac{\tilde{n}\varphi + 2\varphi + 1 + \sqrt{q}}{2} \tag{15a}$$

$$\lambda_2 = \frac{\tilde{n}\varphi + 2\varphi + 1 - \sqrt{q}}{2} \tag{15b}$$

and

$$\vec{v}_1 = \begin{pmatrix} 1 \\ \frac{\tilde{n}\varphi+1+\sqrt{q}}{2\varphi} \end{pmatrix} \tag{16a}$$

$$\vec{v}_2 = \begin{pmatrix} 1 \\ \frac{\tilde{n}\varphi+1-\sqrt{q}}{2\varphi} \end{pmatrix} \tag{16b}$$

where $q = (\tilde{n}\varphi+1)(\tilde{n}\varphi+4\varphi+1)$. From equation (6) and (15a), (15b) it is clear, that λ_1, λ_2 are both positive and that $\lambda_1 > \lambda_2$. Numerical analysis shows, that

$$\frac{\lambda_2}{\lambda_1} \simeq 0.25(\tilde{n}+1)^{-1.5}.$$

Using equatiions (13)–(16) and the diagonalization matrix $\mathbf{Q} = \vec{v}_1\vec{v}_2$, one gets after some calculations

$$\begin{pmatrix} N_w(T_n) \\ N_s(T_n) \end{pmatrix} = \prod_{k=3}^{n+1} N_s(U_k)\mathbf{Q}\begin{pmatrix} \lambda_1^{n-1} & 0 \\ 0 & \lambda_2^{n-1} \end{pmatrix}\mathbf{Q}^{-1}\begin{pmatrix} N_w(T_1) \\ N_s(T_1) \end{pmatrix}. \tag{17}$$

By combining the expressions (17) and (11) the formula for the total number of allowed configurations on the lattice is derived

$$\begin{aligned} N_{total} = \frac{\varphi^3(3+\tilde{n}\varphi)}{\sqrt{q}} \prod_{k=1}^{n+3} N_s(U_k) \Big[&(\varphi\tilde{n}+1)(\varphi+1+\frac{\tilde{n}\varphi}{2})(\lambda_1^{n-1} - \lambda_2^{n-1}) \\ &+ \sqrt{q}(\lambda_1^{n-1}+\lambda_2^{n-1})\Big(1+\frac{\tilde{n}\varphi}{2}\Big)\Big]. \end{aligned} \tag{18}$$

The pair probability $P_n(h_i, h_j)$, which means the probability that at the two lattice sites i, j in a distance n, the column heights are h_i, h_j, is calculated as follows. The equations

(9a)–(9d) give the number of allowed configurations if the column height at the site j is h_j. That means

$$N_{total}(h_i, h_j) = N_s(U_{n+2}) N_s(U_{n+3}) N_s(T_n, h_i) \alpha(h_j, x^*) . \tag{19}$$

In equation (19) $N_s(T_n, h_i)$ is given by (17), with $N_w(T_1)$, $N_s(T_1)$ calculated from (3) with respect to the column height at the site i. The probability $P_n(h_i, h_j)$ is thus

$$P_n(h_i, h_j) = \frac{N_{total}(h_i, h_j)}{N_{total}}$$

and using (17)–(19) we get

$$P_n(h_i, h_j) = \frac{\frac{\alpha(h_j)}{2}\left[\frac{\bar{n}\varphi+1}{\sqrt{q}}(2\beta_w(h_i) + \beta_s(h_i))(\lambda_1^{n-1} - \lambda_2^{n-1}) + \beta_s(h_i)(\lambda_1^{n-1} + \lambda_2^{n-1})\right]}{\frac{\varphi^3(3+\bar{n}\varphi)}{\sqrt{q}}\left[\frac{\bar{n}\varphi+1}{\sqrt{q}}(\varphi + 1 + \frac{\bar{n}\varphi}{2})(\lambda_1^{n-1} - \lambda_2^{n-1}) + \sqrt{q}(\lambda_1^{n-1} + \lambda_2^{n-1})(1 + \frac{\bar{n}\varphi}{2})\right]} \tag{20}$$

which means, that

$$P_{n+1}(h_i, h_j) = \frac{A(\bar{n})\lambda_1^n + B(\bar{n})\lambda_2^n}{C(\bar{n})\lambda_1^n + D(\bar{n})\lambda_2^n} \simeq \frac{A(\bar{n})}{C(\bar{n})}\left[1 + \left(\frac{B(\bar{n})}{A(\bar{n})} - \frac{D(\bar{n})}{C(\bar{n})}\right)\left(\frac{\lambda_2}{\lambda_1}\right)^n\right] \tag{21}$$

where A, B, C, D are numerical constants for certain $\bar{n}$. $P_n(h_i, h_j)$ depends on the column heights at positions i and j, on their distance n and on the amount of dissipated particles $\bar{n}$. For $\bar{n} = 0$ we get the result of Dhar and Majumdar [1]

$$P_n(h_i, h_j) = P(i)P(j) + f_{i,j}4^{-n}$$

where $f_{i,j}$ is a numerical constant.

4. Avalanche size distribution

From the point of view of self-organized criticality, the most important is the power-law character of the avalanche size distribution. For the conservative BTW model on the Bethe lattice, the power-law scaling was derived analytically and, as stated in [1], the avalanche size distribution is

$$g_S \sim S^{-3/2} . \tag{22}$$

The size S of the avalanche is defined by the number of sites hit through one relaxation. Following Dhar and Majumdar [1] I study the probability of the avalanche of size S. In order to get the S-size avalanche on the Bethe lattice, the two conditions must be fulfilled. The sufficient condition reads:

(i) On the connected cluster C_S of S sites, the column height equals to h_{cc}.

The cluster is joined with the trees U_i, $i = 1, 2, \ldots, S+2$. Therefore the second condition is:

(ii) The root sites of these trees must contain less grains then h_{cc}.

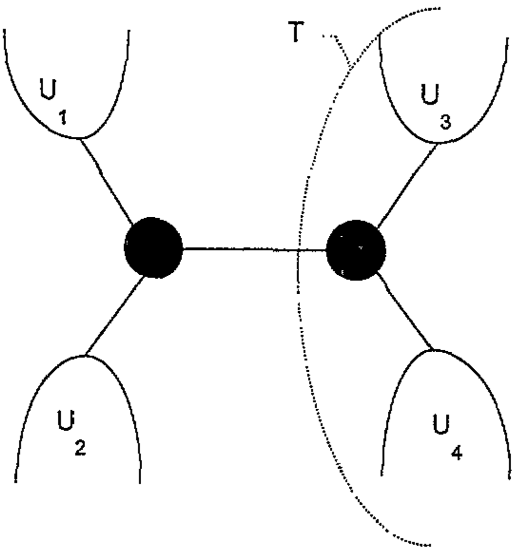

Figure 4. The recursive definition of the two-site cluster (black sites).

Putting accidentally one grain to a certain site lying inside the cluster C_S, the S-size avalanche is triggered. The first step is to calculate the number of allowed configurations containing the cluster C_S. Rewriting the equation (9d) we get for one site cluster C_1

$$N_{C_1} = \prod_{i=1}^{3}(N_s(U_i) + N_w(U_i)). \tag{23}$$

To calculate N_{C_2}, equation (23) is used

$$N_{C_2} = (N_s(T) + N_w(T)) \prod_{i=1}^{2}(N_s(U_i) + N_w(U_i))$$

where T is the tree consisting of U_3, U_4 connected to the site lying in C_2 (figure 4). $N_s(T)$ and $N_w(T)$ are therefore given by (3d) and thus

$$N_{C_2} = \prod_{i=1}^{4}(N_s(U_i) + N_w(U_i)).$$

In the same way also the number of allowed configurations containing S-sized cluster, N_{C_S}, is derived

$$N_{C_S} = \prod_{i=1}^{S+2}(N_s(U_i) + N_w(U_i)) \tag{24}$$

and with respect to condition (ii)

$$N_{C_S} = \prod_{i=1}^{S+2}\left[\sum_{j}^{h_{cc}-1}(N_s(U_i, j) + N_w(U_i, j))\right]. \tag{25}$$

Using equations (3*a*)–(3*d*) and (6), (25) simplifies significantly

$$N_{C_S} = \prod_{i=1}^{S+2} N_S(U_i) \,. \tag{26}$$

As stated in [1], the distribution function

$$g_S = U_S a_S \tag{27}$$

is the multiple of the probability U_S of the configuration C_S which is

$$U_S = \frac{N_{C_S}}{N_{total}} \tag{28}$$

and the number a_S of distinct S sized shapes on the Bethe lattice

$$a_S = \frac{3}{2S+1}\frac{(2S+1)!}{(S+2)!(S-1)!} \,. \tag{29}$$

If N_{C_S} is given by (26) and N_{total} by (17), U_S (28) will be

$$U_S = \frac{\sqrt{q}}{\varphi^3(3+\tilde{n}\varphi)\left[(\varphi\tilde{n}+1)\left(\varphi+1+\frac{\tilde{n}\varphi}{2}\right)(\lambda_1^{S-1}-\lambda_2^{S-1})+\sqrt{q}\left(1+\frac{\tilde{n}\varphi}{2}\right)(\lambda_1^{S-1}+\lambda_2^{S-1})\right]} \,. \tag{30}$$

What we are interested in is the behaviour of the distribution function g_S (27) for great S. In this case

$$U_S \sim \frac{1}{\lambda_1^S} \tag{31}$$

($\lambda_1 > \lambda_2 > 0$, equation (15)) and

$$a_S \sim \frac{4^S}{S^{3/2}} \,. \tag{32}$$

The equations (27), (31) and (32) therefore give g_S for great S

$$g_S \sim \mathrm{e}^{-S/S_0} S^{-3/2} \tag{33}$$

where $S_0 = \log^{-1}\frac{\lambda_1}{4}$. In the conservative model [1] $\tilde{n} = 0$, $\lambda_1 = 4$ (equation (15*a*)) and therefore g_S has a power-law character (22).

5. Results and discussion

I calculated x^*, single site probabilities and the avalanche size distributions for the three versions of the model $(1a)$–$(1c)$. All the expressions derived in the previous sections are general and depending only on the amount of dissipated particles $\tilde{n}$. In the limit $\tilde{n} = 0$ the model $(1a)$–$(1c)$ is conservative and I get the results of Dhar and Majumdar [1], as expected. The numerical results are collected in table 1 and table 2.

It can be seen from table 2, that there is a strong difference in the avalanche size distributions for the conservative ($\tilde{n} = 0$) and non-conservative ($\tilde{n} = 1, 2, 3$) cellular automata. Dissipation causes the exponential drop of g_S and thus incorporates a typical length scale into the distribution. Figure 5 shows a plot of the scale S_0 (33) versus Δ, where Δ denotes that fraction of material, which dissipates to the environment. The dependence has a power-law character, namely $S_0 \sim \Delta^{-1.38}$. this indicates, that the non-conservative

Table 1. Single-site probabilities for the conservative ($\tilde{n} = 0$) and all tree non-conservative versions of the model $(1a)$–$(1c)$. $\tilde{n}$ denotes the number of dissipated particles.

	$P(h_O = 1)$	$P(h_O = 2)$	$P(h_O = 3)$	$P(h_O = 4)$	$P(h_O = 5)$	$P(h_O = 6)$
$\tilde{n} = 0$	$\frac{1}{12}$	$\frac{4}{12}$	$\frac{7}{12}$			
$\tilde{n} = 1$	$\frac{1}{2(3+\sqrt{2}}$	$\frac{11\sqrt{2}-12}{14}$	$\frac{7-3\sqrt{2}}{2(3+\sqrt{2}}$	$\frac{3\sqrt{2}-2}{7}$		
$\tilde{n} = 2$	$\frac{1}{5+\sqrt{17}}$	$\frac{3\sqrt{17}-5}{4(5+\sqrt{17})}$	$\frac{29-3\sqrt{17}}{8(5+\sqrt{17})}$	$\frac{13+5\sqrt{17}}{16(5+\sqrt{17})}$	$\frac{13+5\sqrt{17}}{16(5+\sqrt{17})}$	
$\tilde{n} = 3$	$\frac{9}{46+16\sqrt{7}}$	$\frac{9(\sqrt{7}-1)}{46+16\sqrt{7}}$	$\frac{24-3\sqrt{7}}{46+16\sqrt{7}}$	$\frac{22+10\sqrt{7}}{3(46+16\sqrt{7})}$	$\frac{22+10\sqrt{7}}{3(46+16\sqrt{7})}$	$\frac{22+10\sqrt{7}}{3(46+16\sqrt{7})}$

Table 2. Positive solutions $x^*$of the fixed-point equation (5), eigenvalues λ_1, λ_2 of the transfer matrix $\mathbf{B}$ (14) and the avalanche size distributions for the conservative ($\tilde{n} = 0$) and all tree non-conservative versions of the model $(1a)$–$(1c)$. $\tilde{n}$ denotes the number of dissipated particles.

	x^*	λ_1	λ_2	g_S
$\tilde{n} = 0$	1	4	1	$g_S \sim S^{-3/2}$
$\tilde{n} = 1$	$\sqrt{2} - 1$	4.8284	0.4142	$g_S \sim 0.829^S S^{-3/2}$
$\tilde{n} = 2$	$\frac{\sqrt{17}-3}{4}$	5.8423	0.2807	$g_S \sim 0.685^S S^{-3/2}$
$\tilde{n} = 3$	$\frac{\sqrt{7}-2}{3}$	6.8610	0.2152	$g_S \sim 0.583^S S^{-3/2}$

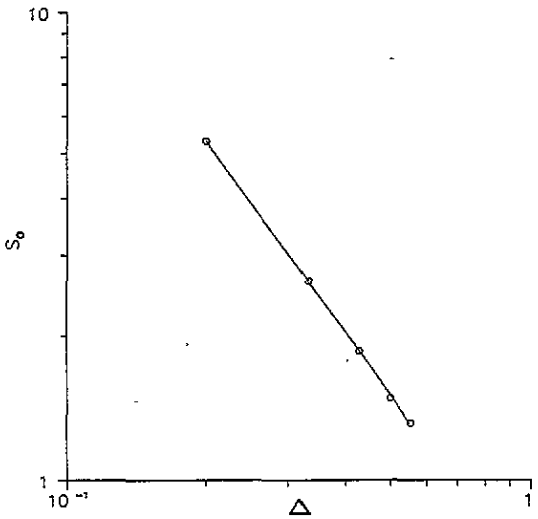

Figure 5. The dependence of the scale S_0 (33) on the fraction of the dissipated material Δ.

randomly driven automata with open boundary conditions defined by (1a)–(1c) cannot reach the SOC state. This is in contradiction to the results found for the open boundary continuously driven models [4, 24], where the power-law avalanche size distributions were found.

The non-conservative model also differs from the conservative one in another property. It was shown [1], that in the conservative cellular automaton, multiple topplings of certain inner site O are rare but possible, and the probability that O topples at least m times, together with the probability P_S that there are exactly S topplings in the avalanche, were calculated analytically. In the model (1a)–(1c) there are no multiple topplings. All the sites topple only once during the avalanche and therefore $P_S = g_S$ for all S.

Acknowledgments

I am grateful to Dr Ľubica Beňušková from the Technical University, Bratislava and Dr Mária Tiňová from the Institute of Measurement SAS, Bratislava for many useful comments.

This work was supported by grant 2/2025/95 of the Slovak Academy of Sciences, and by grant CIPD-CT94-001 (PECO networks program) of the European Community.

References

[1] Dhar D and Majumdar S N 1990 *J. Phys. A: Math. Gen.* **23** 4333
[2] Bak P, Tang C and Wiesenfeld K 1988 *Phys. Rev.* A **38** 364
[3] Kadanoff L P, Nagel S R, Wu L and Zhou S 1989 *Phys. Rev.* A **39** 6524
[4] Grassberger P 1994 *Phys. Rev.* E **49** 2436
[5] Chhabra A B, Feigenbaum M J, Kadanoff L P, Kolan A J and Procaccia I 1993 *Phys. Rev.* E **47** 3099
[6] Grassberger P and Manna S S 1990 *J. Physique* **51** 1077
[7] McNamara B and Wiesenfeld K 1990 *Phys. Rev. Lett.* **65** 1077
[8] McNamara B and Wiesenfeld K 1990 *Phys. Rev.* A **41** 1867
[9] O'Brien K P and Weissman M B 1992 *Phys. Rev.* A **46** R4475
[10] Carlson J M, Chayes J T, Grannon E R and Swindle G H 1990 *Phys. Rev.* A **42** 2467
[11] Chau H F and Cheng K S 1991 *Phys. Rev.* A **44** 6233
[12] Chau H F and Cheng K S 1993 *Phys. Rev.* E **47** 2394
[13] Ivashkevich E V 1994 *J. Phys. A: Math. Gen.* **27** 3643
[14] Ivashkevich E V, Ktitarev D V and Priezzhev V B 1994 *J. Phys. A: Math. Gen.* **27** L585
[15] Dhar D 1990 *Phys. Rev. Lett.* **64** 1613
[16] Dhar D and Ramasvamy R 1989 *Phys. Rev. Lett.* **63** 1659
[17] Markošová M and Markoš P 1992 *Phys. Rev.* A **46** 3531
[18] Markošová M 1995 *Physica* **80D** 41
[19] Nagel S K 1992 *Rev. Mod. Phys.* **64** 321
[20] Puhl H 1992 *Physica* **182A** 295
[21] Reichenbach J 1990 *Phys. Rev. Lett.* **65** 2221
[22] Grinstein G 1991 *J. Appl. Phys.* **69** 8
[23] Grinstein G and Lee D H 1990 *Phys. Rev. Lett.* **64** 1927
[24] Christiansen K and Olami Z 1992 *Phys. Rev.* A **46** 1829
[25] Jánosi I M and Kertézs J 1993 *Physica* **200A** 179
[26] Hwa T and Kardar M 1989 *Phys. Rev. Lett.* **62** 1813